



OPEN Exploring the factors influencing the carbon sink function of coastal wetlands in the Yellow River Delta

Zhixiong Tang^{1,2}, De Wang^{1✉}, Xinpeng Tian¹, Xiaoli Bi¹, Zixiang Zhou², Fubin Luo^{1,2}, Rongrong Ning^{1,2} & Junran Li³

Understanding the mechanisms of the coastal wetland ecosystem carbon sink function is crucial for adapting to, mitigating, and predicting global climate change. Landscape metrics and Carnegie Ames Stanford Approach (CASA) model were used to quantify the spatiotemporal patterns of soil organic carbon (SOC) and vegetation carbon sequestration (VCS) in the Yellow River Delta (YRD). GeoDetector model was used to explore the effects of various factors influencing VCS. The results showed that: (1) From 1999 to 2020, the area of natural wetlands and non-wetlands decreased, while the area of artificial wetlands increased. (2) The SOC stock in the 0~100 cm depth in 1999 and 2020 were about 7.8871 Tg C and 7.0521 Tg C, respectively. The amount of VCS increased from 0.2309 Tg C in 2000 to 0.3681 Tg C in 2020, with a significant annual increase of 6532 Mg C. In the past 21 years, the total carbon sink in the YRD was 6.0952 Tg C. The amount of VCS was equivalent to 2.93% of SOC stock in 1999, rising to 5.22% by 2020. (3) Vegetation cover has the greatest influence on the carbon sink function in the YRD, followed by precipitation and biodiversity. From 2000 to 2020, the effect of biodiversity on the carbon sinks of natural wetlands and artificial wetlands increased. The synergistic effect of wetland type and vegetation cover on carbon sink effect was replaced by the synergistic effect of biodiversity and vegetation cover. The identification of the primary factors that influence VCS in the YRD is significant to the understanding of the spatiotemporal evolution of carbon sink effect in coastal wetland ecosystems, and to the guidance of the rational development and protection of coastal wetlands and promote sustainable ecosystem development.

Keywords Coastal wetlands, Soil organic carbon, Vegetation carbon sequestration, Influencing factor, Yellow River Delta

According to the latest report of the Intergovernmental Panel on Climate Change (IPCC), the massive increase in carbon emissions is responsible for causing approximate warming of 1.1 °C above pre-industrial levels¹. The consequences of global warming, including the rising sea levels and the increased frequency of extreme weather events, have posed a significant threat to the sustainability of ecosystem services^{2,3}. Consequently, there is an urgent need to mitigate the negative effects of the greenhouse effect⁴. The atmospheric carbon dioxide (CO₂) is fixed by ecosystems in plants and soil through the process of photosynthesis in vegetation, which has the potential to mitigate global warming⁵. Understanding the mechanisms of the ecosystem carbon cycle is crucial for adapting to, mitigating, and predicting global climate change⁶.

Vegetation carbon sequestration (VCS) refers to the mechanisms or processes that absorb and fix CO₂ from atmosphere through photosynthesis⁷. The main drivers of VCS include vegetation cover, climate change, topography, and geomorphology. Vegetation type, which is influenced by natural conditions and human activities, has a very important positive effect on the VCS^{8–10}. Large-scale ecological projects can promote regional greening to mitigate the greenhouse effect^{11,12}. The respiration and photosynthesis of vegetation are subject to influence from climatic variables such as temperature and precipitation, which consequently affect the VCS¹³. Different vegetation types on different terrains and landforms affect the function of the VCS. The carbon sequestered by vegetation through photosynthesis returns directly to the soil surface with litter, and most of it is fixed in the soil as soil organic carbon (SOC)¹⁴. SOC is the largest carbon reservoir in terrestrial ecosystems¹⁵. Global SOC stock is about 234.4 billion tons, 54% of which is stored in the first meter of soil, and small changes in storage can have an impact on atmospheric concentrations of CO₂^{14,16,17}. The effect of vegetation type on

¹Yantai Institute of Coastal Zone Research, Chinese Academy of Sciences, Yantai 264003, China. ²College of Geomatics, Xi'an University of Science and Technology, Xi'an 710054, China. ³Department of Geography, The University of Hong Kong, Hong Kong 999077, SAR, China. ✉email: dwang@yic.ac.cn

SOC density cannot be ignored^{14,18}. Therefore, it is necessary to explore the SOC and VCS and their influencing factors as a whole when exploring the carbon sink function in ecosystems.

The anaerobic environment of coastal wetlands is not conducive to aerobic decomposition of organic matter and has higher vegetation primary productivity and VCS rate than terrestrial ecosystems¹⁹. At the same time, coastal wetland ecosystems have a relatively high SOC density, covering only 0.3% of the Earth's surface but contributing 20–25% of the terrestrial SOC stocks^{20,21}. Glacier melting and sea level rise caused by the greenhouse effect will lead to the disappearance of 20%–90% of coastal wetland ecosystems². At present, the scientific community agrees that ecosystems in China are important carbon sinks^{22–24}. China's coastal wetlands account for about 1/4 of the total area of coastal wetlands in the world²⁵. Over the past four decades, the area of the total coastal wetland in China and their associated carbon sink have declined²⁶. The exact factors that may influence such a decline in carbon sink, and the relative significance of these factors, however, are still unknown.

The Yellow River (YR) was once the second largest river of the world in terms of sediment delivery to the sea, with an annual load of 1.08 Gt / yr²⁷. The Yellow River Delta (YRD), located at the mouth of the YR, is the most complete coastal wetland ecosystem in the warm temperate zone of China (Fig. 1). In 2002, the Yellow River Conservancy Commission launched the water-sediment regulation scheme (WSRS), which aims to alleviate siltation in reservoirs and downstream riverbeds²⁸. The WSRS allows approximately 30% of the water and 50% of the sediment that passes through the YRD to be discharged to the sea in a short period of time, significantly altering the natural seasonal rhythm of the hydrological cycle²⁷. Since the initial implementation of the WSRS, wetland areas have increased in the YRD but decreased in habitat quality (HQ)²⁹, which significantly impacted carbon cycle in the YRD³⁰. Meanwhile, parts of the YRD are suffering from brine over-exploitation³¹ and land subsidence³², which further altered the patterns of land use/cover (LUC). The unique geographic location and natural conditions make the YRD an important research target for understanding the carbon cycle in coastal wetlands. Many current studies have investigated VCS stocks and VCS rate through research methods such as field sampling^{33,34}, remote sensing inversion^{35–38}, and controlled experiments^{39–42}. Furthermore, some studies have investigated the stocks^{43–45}, distribution characteristics⁴⁶ and their influencing factors^{47–52} of SOC in the YRD, utilizing measured data or landscape pattern estimation.

To summarize, for decades, scientists have conducted related studies to explore the carbon sink effect in the YRD. However, the majority of previous research were limited. Some of the gaps in the current knowledge can be summarized as follows: (1) Most of the researches have investigated only the stocks and influencing factors of a single carbon pool (vegetation or soil) in the YRD. (2) In terms of a temporal scale, few studies followed a long, continuous timeline (over 20 years). Most existing research is limited to a short period. (3) The existing studies on the influencing factors of carbon sinks do not consider the role of trade-offs between these factors. (4) The mechanisms influencing the carbon sink effect of vegetation in different LUCs have been the subject of only a limited number of studies. The objective of our study was to investigate factors that may affect the dynamics of carbon sinks, and their relative importance in the YRD for a period over 20 years. We hypothesized that total carbon sink has changed with the decrease of nature wetlands area in the YRD area, but this process may be complicated by the addition of artificial wetlands and change in plant diversity in the past two decades. The present study seeks to answer: (1) What are the characteristics of land use/cover change (LUCC)? (2) What are the characteristics of SOC and VCS changes? (3) What has changed in the mechanism of influence of the VCS?

To the best of our knowledge, this paper systematically evaluates SOC and VCS over the last 20 years in YRD, and explores the factors influencing carbon sinks. Furthermore, this study is the first to investigate changes in the influence mechanisms of VCS in different LUC types over the past two decades, all of which are gaps in the literature that we try to fill in this paper. The results can not only help to better understand the spatiotemporal evolution of carbon sink effect in coastal wetland ecosystems, but also guide the rational development and protection of coastal wetlands and promote sustainable ecosystem development.

Materials and methods

Study area

The YRD (118°33'E ~ 119°21'E, 37°35'N ~ 38°12'N), located between Laizhou Bay and Bohai Bay (Fig. 1), covers an area of about 3,000 km² and is an important oil and energy base for China. The YRD is an alluvial plain formed at the mouth of the YR into the sea. It faces severe land subsidence due to its extremely young geology³². The YRD is located at the boundary between sea and land, with a gentle slope, and is the most complete coastal wetland ecosystem in the warm temperate zone of China. The average annual temperature of the YRD is 11.5 to 12.4 °C, and the average annual precipitation ranges from 530 to 630 mm.

Data sources

The data used in this study include: (1) LUC data (1999, 2004, 2009 and 2013) were obtained according to Li⁵³. LUC data for 2017 and 2020 were obtained using the same remote sensing interpretation method. The dataset has a spatial resolution of 30 m, and adopts the wetland classification system established by Li⁵³ for the unique location environment of the YRD. The accuracy of the interpretation was verified to be more than 80% in all periods, as demonstrated by the accuracy verification of the validation sample point data collected from the field trip²⁹. The LUC types included four first-level classes: natural-wetlands (Wna), artificial wetlands (War), non-wetlands (Wno) and Ocean, and 19 s-level classes. (2) Soil sampling data were provided by the Institute of Geographical Sciences and Natural Resources Research: based on the grid distribution point method, 145 samples were collected in 2002 and 94 samples were collected in 2003 at 0 ~ 10, 10 ~ 30, 30 ~ 60 and 60 ~ 100 cm soil depths. The samples were evenly distributed in space, with an average spacing of about 6 km. (3) The sunshine duration dataset (2000 ~ 2020) was obtained from China Meteorological Data Sharing Service Network (<https://data.cma.cn/>), and the daily solar radiation dataset was simulated by SWAT weather generator; The temperature

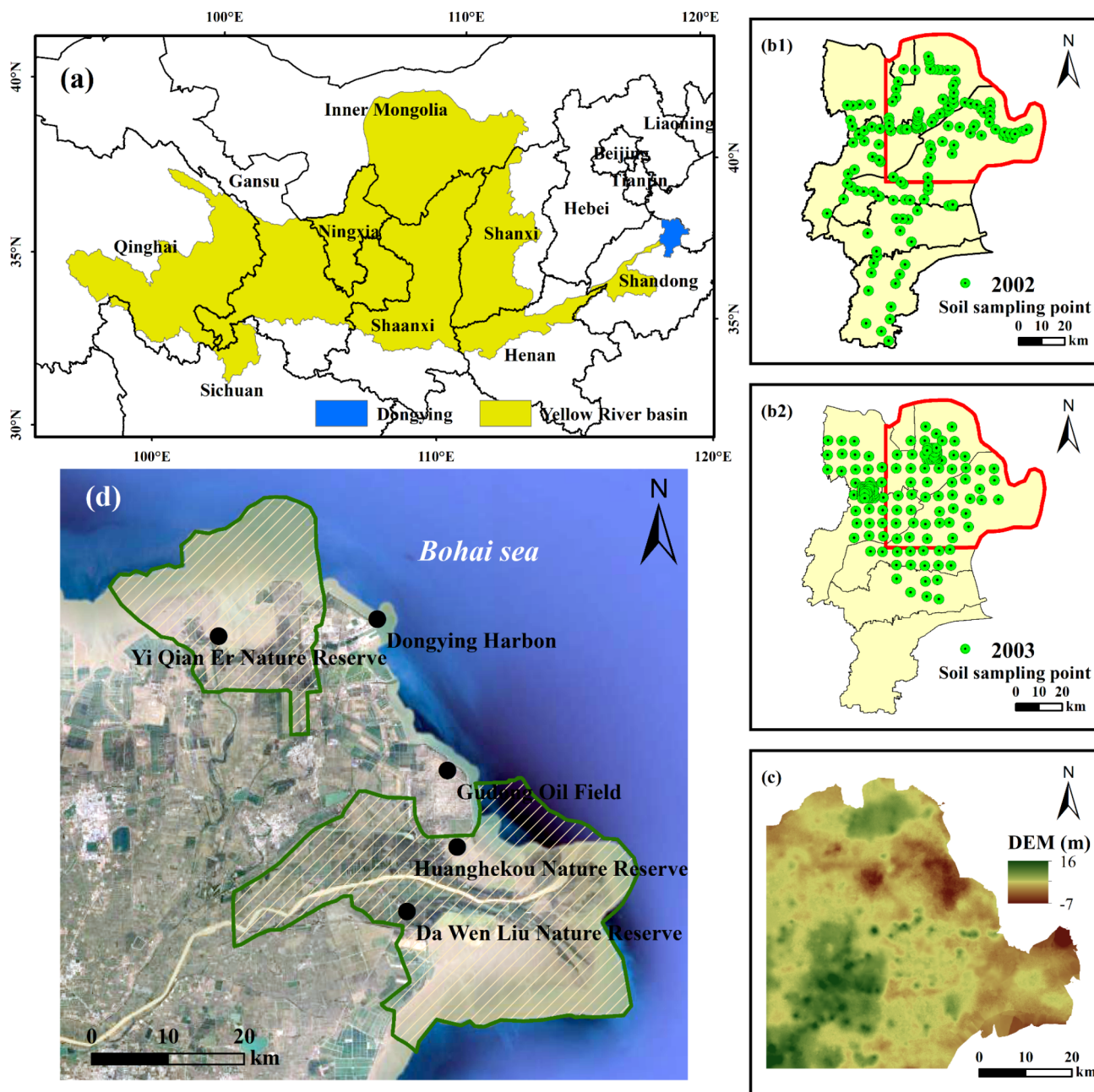


Fig. 1. Location of the YRD (**a**: The location of Dongying City; **b1** and **b2**: Location of soil sampling points; **c**: DEM of the YRD; **d**: Sentinel-1 A image of the YRD and boundary of the Yellow River Delta National Nature Reserve). Note: This figure was generated by ArcMap 10.0 (<https://support.esri.com/en/products/desktop/arcgis-desktop/arcmap>).

dataset (2000~2020) was the GPRChinaTemp1km dataset produced by He et al.⁵⁴; The precipitation dataset (2000~2020) was the national 1 km spatial resolution monthly precipitation dataset produced by Qu et al.⁵⁵. (4) DEM provided by the National Aeronautics and Space Administration (NASA) (<https://www.earthdata.nasa.gov/>). (5) NDVI data from MODIS13Q1 were obtained from NASA (<https://www.earthdata.nasa.gov/>). The spatial resolution was 250 m and the temporal resolution was 16 days. (6) HQ data obtained according to Tang²⁹.

Research methods

Soil organic carbon

The study of SOC in the YRD region employed the use of density, content, and stock as key indicators^{44,56–58}. The SOC content, SOC density and SOC stock were calculated as Eqs. (1), (2) and (3), respectively.

$$SOCc_i = B_i \times O_i \times 0.58 \quad (1)$$

$$SOCd_j = \sum H_i \times SOCc_i \quad (2)$$

$$SOCs = \sum SOCd_j \times A_j \quad (3)$$

where: i is soil layer; j is land use/cover type; $SOCc$ is soil organic carbon content (kg/m^3); $SOCd$ is soil organic carbon density (kg/m^2); H_i is the soil layer height of layer i (m); B_i is soil bulk density (kg/m^3); O_i is soil organic matter content (%); 0.58 is the Bemmelen index that converts organic matter concentration to organic carbon content because organic matter was calculated by wet combustion with $\text{Cr}_2\text{O}_7^{[-2]}$ ⁵⁹; $SOCs$ is soil organic carbon stock (kg); A is the area of various land use/cover types (m^2).

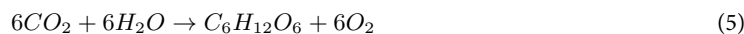
Vegetation carbon sequestration

The Carnegie Ames Stanford Approach (CASA) model fully considers the environmental conditions and the characteristics of vegetation, and estimates the net primary productivity (NPP) by simulating the photosynthetic active radiation absorbed by plants and the actual utilization of light energy⁶⁰. In this paper, the improved CASA model is used to simulate the spatiotemporal pattern of NPP in the YRD from 2000 to 2020^{13,61}. The expressions are as follows:

$$NPP(x, t) = APAR(x, t) \times \varepsilon(x, t) \quad (4)$$

where: x is the pixel; t is the month; NPP is the net primary productivity (gC/m^2); $APAR$ is the photosynthetic effective radiation absorbed (MJ/m^2); ε is a factor that reflects the efficiency with which light energy is used to produce organic compounds (gC/MJ). In comparison with other studies, the values of our NPP were within a reasonable range (Table 1).

According to the photosynthetic reaction equation, the production of 1 kg of dry matter can fix 1.63 kg CO_2 . Then, according to the ratio of the relative molecular masses of carbon and CO_2 , it can be known that 1 kg CO_2 contains 12/44 kg of carbon elements⁶¹. We calculated the amount of VCS by combining the amount of NPP material (the production of dry matter in an ecosystem) with the photosynthetic reaction equation. To approximate carbon sink, the amount of VCS was used.



$$VCSr = NPP \times 1.63 \times 12/44 \quad (6)$$

$$VCSs = \sum VCSr_x \times A_x \quad (7)$$

where: $VCSr$ indicates the vegetation carbon sequestration rate per unit area corresponding to the ecosystem; $VCSs$ represent vegetation carbon sequestration stock; x is the pixel; A is the area of various land use/cover types.

GeoDetector model

GeoDetector is a new statistical method used to reveal the main driving factors of spatial differentiation of certain geographical phenomena. GeoDetector model has been demonstrated to be effective in studying the factors that influence carbon sink effects⁶¹. In this study, with the help of FactorDetector and InteractionDetector of GeoDetector, the main influencing factors of carbon sink are identified^{61–63}.

- FactorDetector. FactorDetector is a measure of the spatial differentiation characteristics of the dependent variable and the spatial differentiation characteristics of the independent variable on the dependent variable through Q values^{64,65}. The Q value is calculated in Eq. 8:

$$Q = 1 - \frac{\sum_{m=1}^L N_m \sigma_m^2}{N \sigma^2} \quad (8)$$

where: N is all sample numbers; $m = 1, 2, \dots, L$ denotes a sub-area; N_m is the number of samples in the m -th sub-area, σ^2 is the variance of the VCS rate.

- InteractionDetector. InteractionDetector compares the sum of the influence of the two influencing factors on the carbon sink with the influence of the two influencing factors when combined. In this paper, we use InteractionDetector to explore whether the two influencing factors (F1 and F2) weaken or enhance each other's influence when they are together, or whether they are independent (Table 2)^{64,65}.

Annual NPP (gC/m^2)	Area	Method/data	Time	References
215.328	YRD	CASA	2000~2020	This study
208.291	YRD	BIOME-BGC	2000~2020	MOD17A3
294.380	YRD	CASA	2016~2017	Chi et al. ³⁵

Table 1. The NPP values obtained in this study were compared with those of other studies.

Judgment	Interaction
$Q(F1 \cap F2) > Q(F1) \text{ or } Q(F2)$	Enhance
$Q(F1 \cap F2) > Q(F1) \text{ and } Q(F2)$	Enhance; bivariate
$Q(F1 \cap F2) > Q(F1) + Q(F2)$	Enhance; nonlinear
$Q(F1 \cap F2) < Q(F1) + Q(F2)$	Weaken
$Q(F1 \cap F2) < Q(F1) \text{ or } Q(F2)$	Weaken; univariate
$Q(F1 \cap F2) < Q(F1) \text{ and } Q(F2)$	Weaken; nonlinear
$Q(F1 \cap F2) = Q(F1) + Q(F2)$	Independent

Table 2. The judgment basis for InteractionDetector (F1 and F2 represent two different influencing factors).

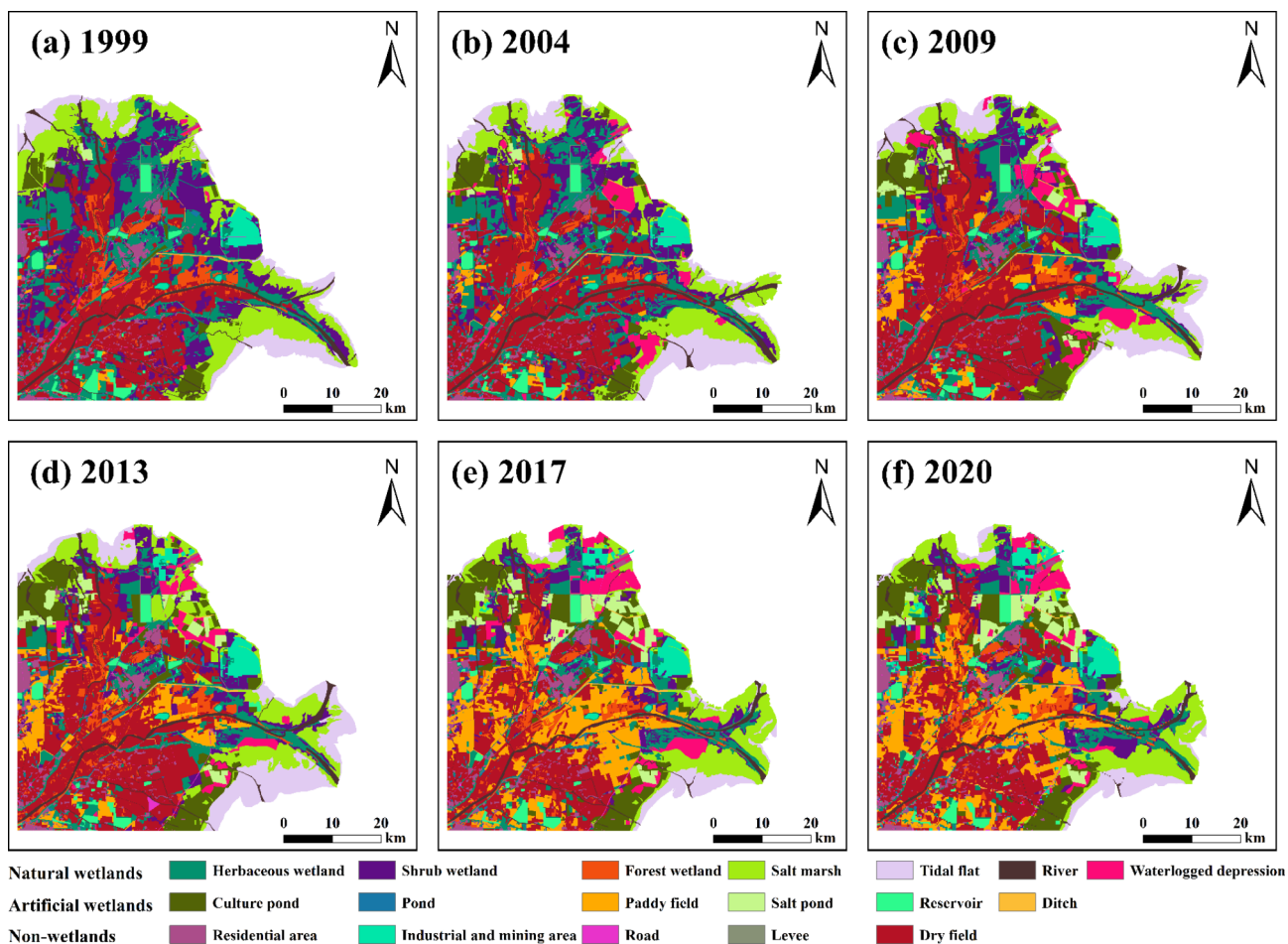


Fig. 2. Spatial pattern of LUC in the YRD from 1999 to 2020. Note: This figure was generated by ArcMap 10.0 (<https://support.esri.com/en/products/desktop/arcgis-desktop/arcmap>).

In addition to NDVI and meteorological factors, the influencing factors of carbon sink include DEM, Slope, LUC, HQ and other geographical factors. Using the GeoDetector model, we explored the factors influencing the carbon sink in the YRD area from 2000 to 2020. Among the influencing factors considered, Slope and DEM were selected as the limiting factors for Wno expansion. HQ was selected as an indicator of biodiversity change characteristics.

Results

Spatiotemporal variations characteristics of LUC

The coastal wetland ecosystem of the YRD is mainly Wna. In 1999, the areas of Wna, War and Wno were 1964.498 km², 179.815 km² and 867.853 km² respectively. In 2020, the areas of Wna, War and Wno were 1201.295 km², 931.973 km² and 850.229 km², respectively (Figs. 2 and 3).

The LUC types in the YRD changed significantly from 1999 to 2020. Among which the Wna area showed a significant reduction trend, which reduced about 763.203 km², with reduction ratios of 38.9%. The area of

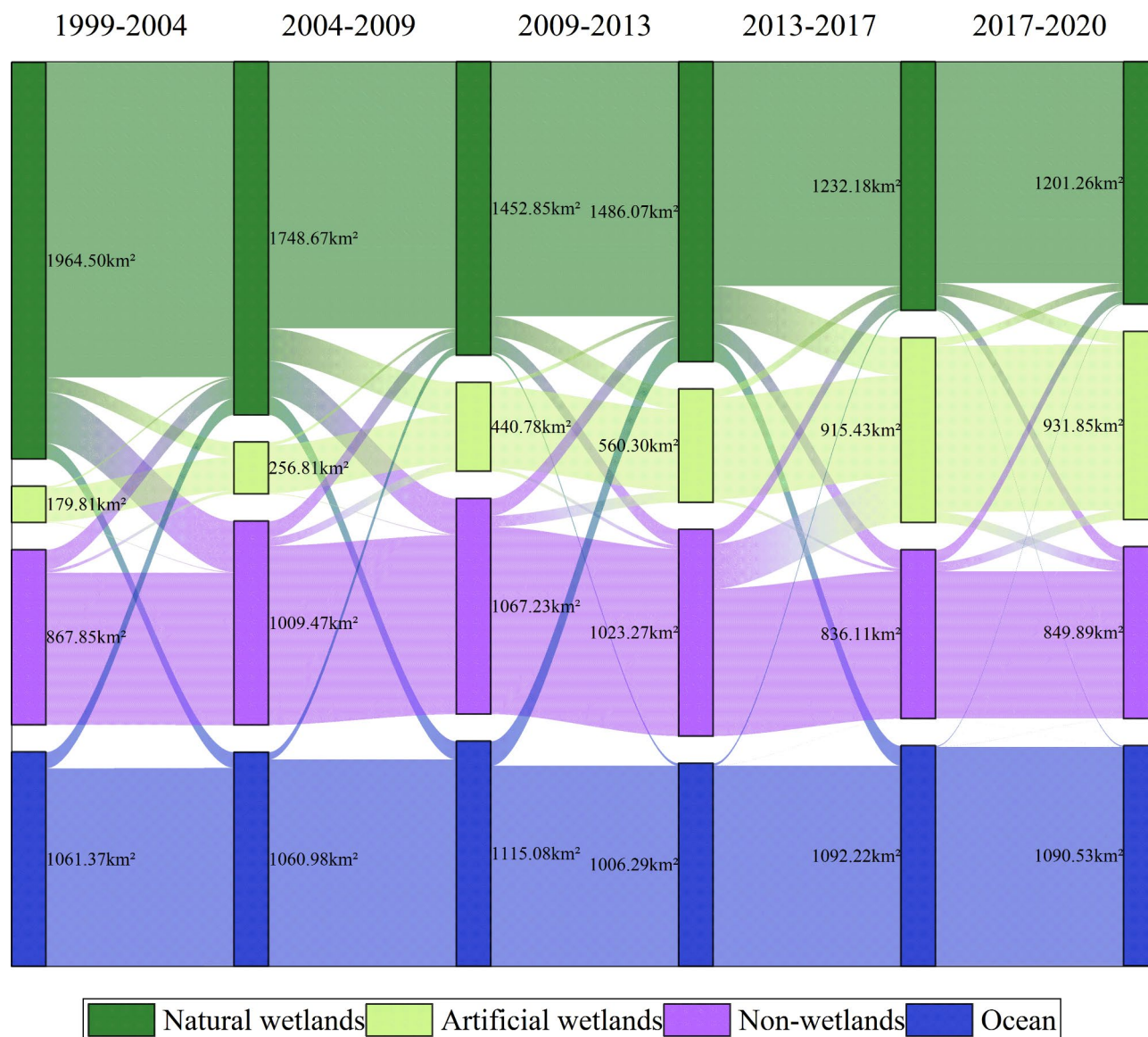


Fig. 3. Direction of transfer between different LUC in the YRD from 1999 to 2020.

Wno only decreased by about 17.624 km², a reduction rate of 2.0%. On the contrary, War expanded about 752.158 km² with an expansion rate of 418.3%.

As can be seen from Figs. 3 and 72.1% of War, 95.8% of Wno and 99.9% of ocean expansion area come from encroaching Wna. In addition, War, Wno and ocean accounted for 7.2%, 47.6% and 45.2% of the total area transferred to Wna, respectively. This indicates that human activities are the main reason for the dynamic change of Wna area in the YRD. We also found that 57.2% of the transferred area of Wna and 67.5% of the transferred area of Wno were mainly transferred to War, 56.7% of the transferred area of War and 99.3% of the transferred area of ocean were mainly transferred to Wna.

Spatiotemporal variations characteristics of SOC

The average SOC density in the YRD was 2.898 kg/m², and the spatial heterogeneity of SOC density was obvious in different soil layers. The deeper the soil layer in the YRD, the smaller the SOC content. The spatial pattern of SOC content in different soil layers of the YRD is shown in Fig. 4. The average SOC content in the 0~10 cm, 10~30 cm, 30~60 cm and 60~100 cm layers were 7.731 kg/m³, 3~5 kg/m³, 2.466 kg/m³ and 1.657 kg/m³, respectively. Further analysis showed that the SOC content of 0~10 cm soil in the YRD was much higher than that in other soil layers.

According to the soil sampling data, Eq. (3) was used to estimate the SOC stock in different soil layers from 1999 to 2020 (Table 3). The results showed that the SOC stock in the 0~100 cm depth in 1999, 2004, 2009, 2013 and 2020 were about 7.8871 Tg C, 7.5785 Tg C, 7.1661 Tg C, 7.4453 Tg C, and 7.0521 Tg C, respectively, indicating that the SOC stock showed a decreasing trend in non-linear fluctuations from 1999 to 2020.

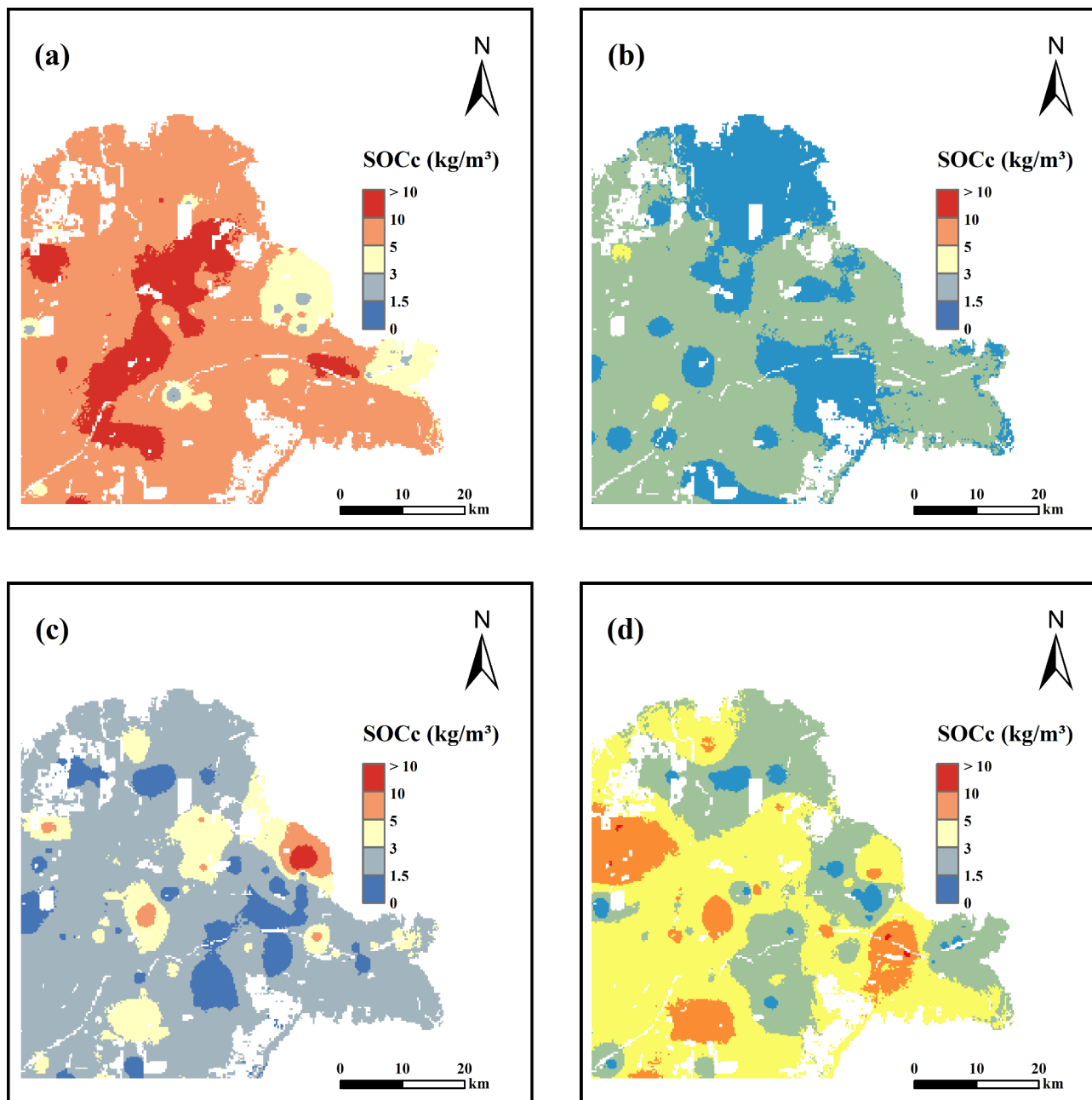


Fig. 4. The distribution of SOC content in YRD (a: 0 ~ 10 cm; b: 10 ~ 30 cm; c: 30 ~ 60 cm; d: 60 ~ 100 cm). Note: This figure was generated by ArcMap 10.0 (<https://support.esri.com/en/products/desktop/arcgis-desktop/arcmap>).

Spatiotemporal variations characteristics of VCS

We first examined the VCS rate per unit area in the YRD (Fig. 5a), which showed an increasing trend during the period 2000 ~ 2020. The VCS rate increased from 78.233 g/m² in 2000 to 126.099 g/m² in 2020, with a significant annual increase of 2.273 g/m² ($P < 0.01$). It is worth noting that the growth rate of Wno was the fastest, and the growth rate of Wna was less than that of War. From a quarterly trend (Fig. 5b), the change trend of each quarter was consistent with the interannual trend. In addition, the contribution of spring, summer, autumn and winter to annual VCS reached 12.10%, 57.89%, 22.88% and 7.13% respectively, which indicated that the vegetation carbon sink in the YRD mainly occurred in summer.

The annual average VCS rate per unit area in the YRD ranges from 0.328 g/m² to 360.064 g/m², with high values mainly distributed along the river channel and low values mainly distributed near the coastal zone (Fig. 6a). In addition, we used the MK-Sen method to explore the spatial distribution of the VCS rate variation trend (Fig. 6b). It increased significantly in the YRD, War and Wno, while it did not increase significantly in Wna (Table 4).

Data		Years					
		1999	2004	2009	2013	2017	2020
SOC stock	00–10 cm	2.1109	2.0269	1.9153	1.9703	1.8318	1.8435
	10–30 cm	1.9360	1.8734	1.7742	1.8458	1.7379	1.7519
	30–60 cm	2.0352	1.9400	1.8273	1.9191	1.7897	1.8376
	60–100 cm	1.8049	1.7383	1.6493	1.7101	1.6029	1.6190
	0–100 cm	7.8871	7.5785	7.1661	7.4453	6.9623	7.0521
VCS stock	Wna	1.327	1.715	1.496	1.233	1.031	1.251
	War	0.119	0.134	0.291	0.364	0.792	1.052
	Wno	0.863	1.299	1.432	1.183	1.013	1.379
	YRD	2.309	3.147	3.220	2.780	2.837	3.681

Table 3. SOC stock in different soil layers and VCS stock in different LUC (tg C). Wna: natural wetlands; War: artificial wetlands; Wno: non-wetlands. The VCSs in 1999 was based on the NPP data in 2000 and was calculated from the LUC in 1999.

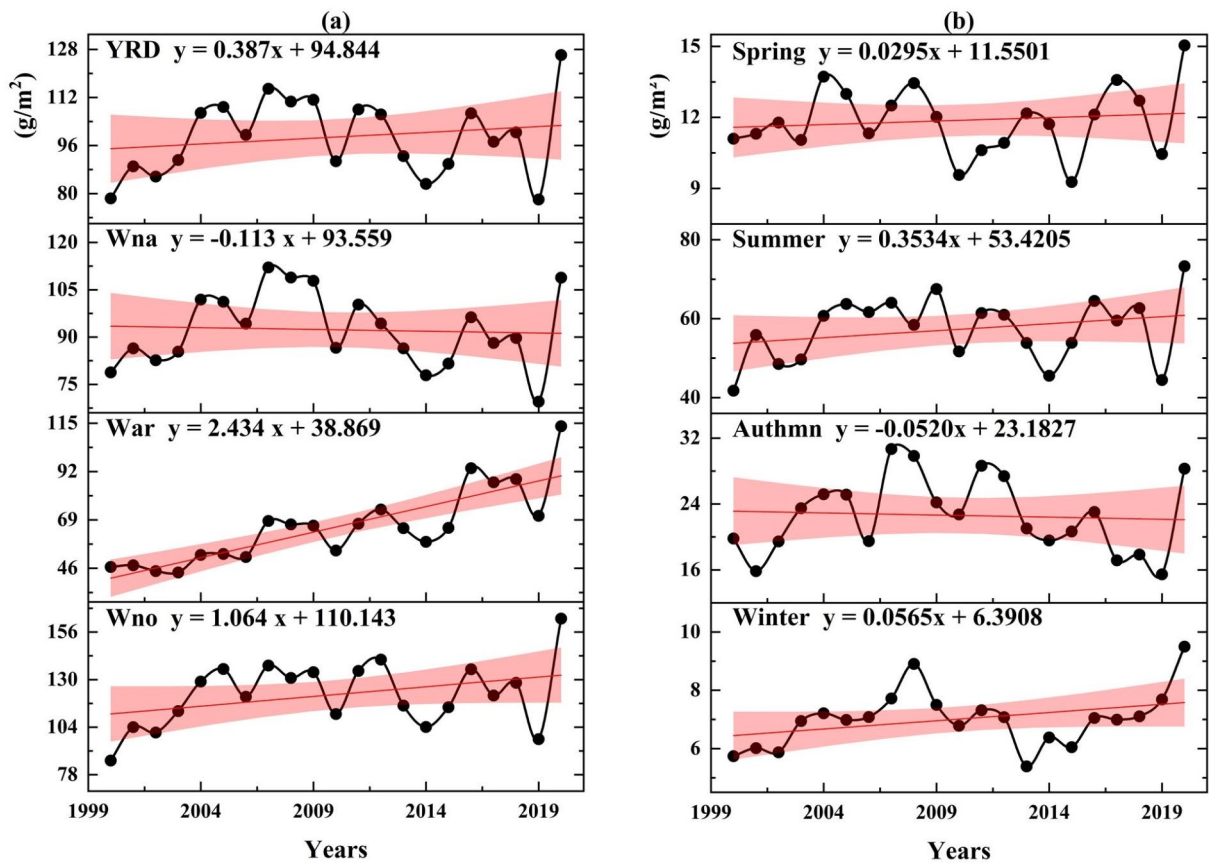


Fig. 5. Interannual variation trend of VCS (a: the trend of VCS rate in different LUC; b: the trend of VCS rate in different seasons).

In terms of temporal evolution, from 2000 to 2020, the amount of VCS in the YRD showed an increasing trend (Table 3). The amount of VCS increased from 0.2309 Tg C in 2000 to 0.3681 Tg C in 2020, with a significant annual increase of 6532 Mg C. In 21 years, the total carbon sink in the YRD was 6.0952 Tg C. The amount of VCS was equivalent to 2.93% of SOC stock in 1999, but it has increased to 5.22% by 2020.

The amount of VCS of Wna decreased from 2000 to 2020, showing a decreasing trend (Table 3). The total carbon sink of Wna in 21 years was 2.7883 Tg C, and the amount of VCS decreased from 0.1327 Tg C in 2000 to 0.1251 Tg C in 2020, decelerating to 363 Mg C per year, and its proportion in the amount of VCS of YRD decreased from 57.45 to 33.97%. The total carbon sink of War in 21 years was 0.7917 Tg C, and the amount of VCS increased from 0.0119 Tg C in 2000 to 0.1052 Tg C in 2020, increasing to 4440 Mg C per year, and its

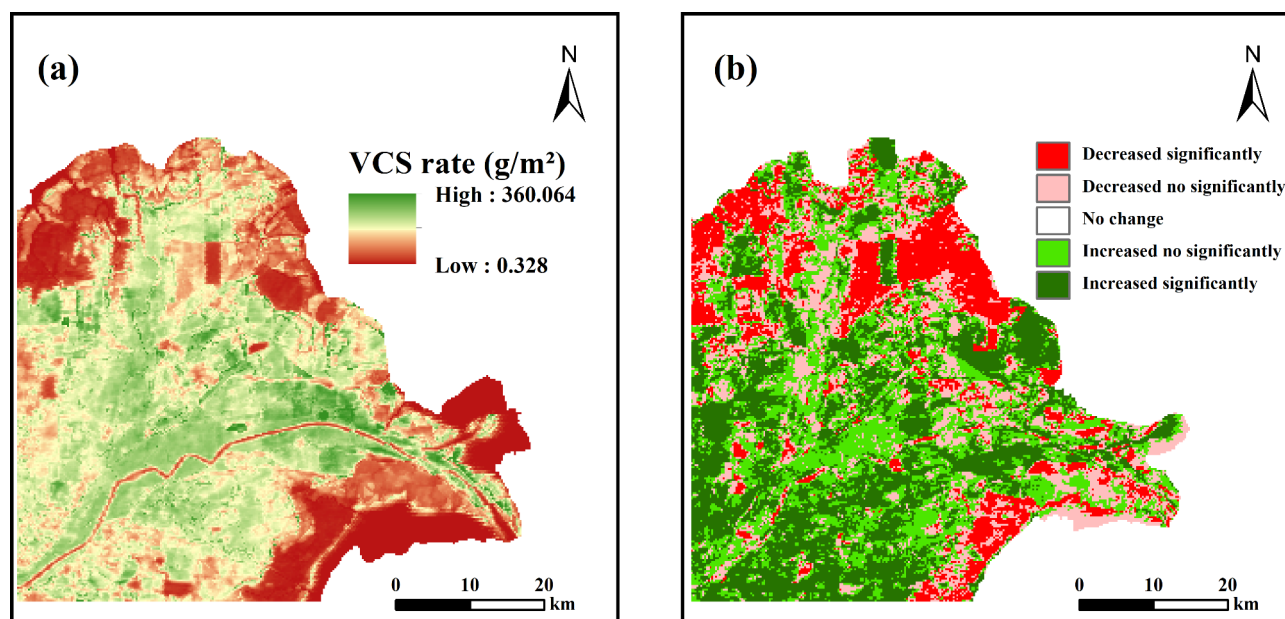


Fig. 6. Spatial distribution and variation trends of VCS rate from 2000 to 2020 in the YRD (**a**: the spatial pattern; **b**: the variation trend). Note: This figure was generated by ArcMap 10.0 (<https://support.esri.com/en/products/desktop/arcgis-desktop/arcmap>).

Variation trends	Increased significantly	Increased no significantly	No change	Decreased no significantly	Decreased significantly
YRD	29.58	27.38	5.70	20.68	16.65
Wna	22.21	25.57	13.21	23.33	15.69
War	28.70	24.13	0.42	19.44	27.31
Wno	41.20	33.67	0.39	18.36	6.37

Table 4. Proportion of variation trends of the VCS rate per unit area by LUC type (%). Wna: natural wetlands; War: artificial wetlands; Wno: non-wetlands.

proportion in the amount of VCS of YRD increased from 5.16 to 28.57%. The total carbon sink of Wno in 21 years was 2.5512 Tg C, and the amount of VCS increased from 0.0863 Tg C in 2000 to 0.1379 Tg C t in 2020, increasing to 2455 Mg C per year, and its proportion in the amount of VCS of YRD increased from 37.39 to 37.46%. Wna was the main contributor to the VCS in the YRD in 2000 and was converted to Wno in 2020.

Influencing factor of carbon sinks in different LUC types

Vegetation cover, temperature and precipitation are important factors affecting ecosystem carbon sinks. The interannual changes of VCS rate, NDVI, temperature and precipitation of YRD were compared (Figs. 5 and 7). The trends of NDVI and VCS rate were highly similar, decreasing in 2009 ~ 2010, 2012 ~ 2014 and 2018 ~ 2019. The trend of VCS rate and precipitation and VCS rate both fluctuated and increased, but the similarity of the trend in some years was not high.

The YRD area exhibited an increase in temperature and a decrease in precipitation in 2014 and 2016, followed by a decrease in temperature and an increase in precipitation in 2018 and 2020. The temporal variation trends of NDVI on different LUC types were inconsistent, and the multi-year average NDVI of Wno was the largest (Fig. 7a). This is attributable to the considerable proportion of dryland area in Wno, which consistently exceeds 70%, and the elevated NDVI values observed in drylands. The average NDVI of War was smaller than that of Wna in 2000 and greater than that of Wna in 2020. The interannual trends of temperature and precipitation on different LUC types were generally consistent with the interannual trends in the YRD.

Since 2000, the VCS rate of the YRD has been changing continuously under the influence of vegetation restoration and climate change. We compared the correlation between VCS rates and NDVI and meteorological factors in the YRD from 2000 to 2020 (Table 5). The results indicated that the VCS rate was mainly insignificant correlated with NDVI, precipitation, or temperature.

The key findings (Fig. 8a1&b1) were: (1) From 2000 to 2020, NDVI had the most significant effect on the carbon sink of YRD. Its Q values were the highest (0.4432 and 0.7190, respectively). The influencing factor ranking was followed by precipitation and HQ. Q values for precipitation were 0.1399 and 0.1952, respectively. Q values for HQ were 0.1287 and 0.1403, respectively. Q values for Slope were lower than the other factors. (2) The influence of DEM and temperature increased, while the importance of LUC decreased. In 2000, the influence

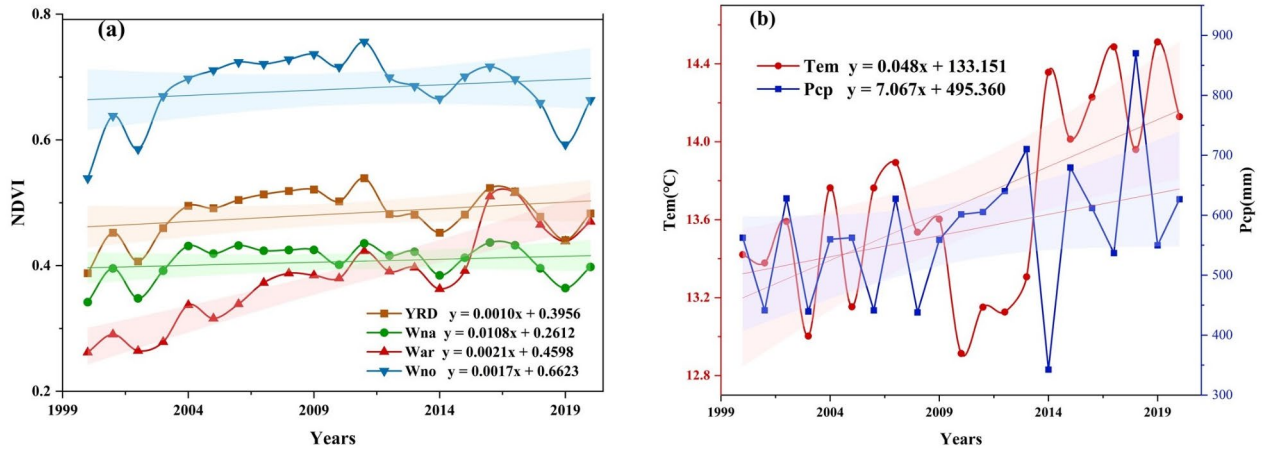


Fig. 7. Time change trend of influencing factor (a: Interannual variation of NDVI in different LUC types; b: Interannual variations in temperature and precipitation).

Influencing factor	LUC types	Significant correlated	Insignificant correlated	No change	Insignificant irrelevant	Significant irrelevant
VCS rate & NDVI	YRD	0.13	94.94	3.15	1.62	0.15
	Wna	0.19	89.36	7.60	2.60	0.24
	War	0.11	97.81	0.38	1.55	0.15
	Wno	0.08	99.11	0.35	0.42	0.04
VCS rate & temperature	YRD	1.43	49.97	2.34	44.86	1.39
	Wna	1.29	48.14	5.50	43.68	1.38
	War	1.20	45.35	0.38	51.86	1.21
	Wno	1.86	57.45	0.35	38.73	1.61
VCS rate & precipitation	YRD	1.43	63.40	2.34	31.36	1.47
	Wna	1.51	58.71	5.50	32.73	1.54
	War	1.51	55.10	0.38	41.57	1.44
	Wno	1.22	78.66	0.35	18.36	1.41

Table 5. The correlation of the influencing factor (%). Wna: natural wetlands; War: artificial wetlands; Wno: non-wetlands.

was ranked as LUC > DEM > temperature, and in 2020, the influence was ranked as DEM > temperature > LUC. (3) The synergy between LUC and NDVI played important role in 2000; the synergy between HQ and NDVI played important role in 2020.

Furthermore, the effects of each influencing factor on the carbon sink effect of Wna, War and Wno were explored. In 2000, the dominant factor was NDVI, followed by precipitation. Compared with Wna and War, temperature had a greater influence on Wno, and HQ had a smaller influence on Wno (Fig. 8a2-a4). By 2020, the dominant factor on Wna and War was NDVI, followed by HQ. The dominant factor on Wno was NDVI, followed by precipitation; Compared with Wna and War, temperature had a greater influence on Wno, and HQ had a smaller influence on Wno (Fig. 8b2-b4). The synergy between HQ and NDVI had a significant influence on the VCS of each LUC type between 2000 and 2020.

Discussion

Impacts of land use structure on carbon sink effect

The spatiotemporal variation of SOC stock is closely related to the evolution of the YRD. Table 3 indicating that the SOC stock showed a decreasing trend in non-linear fluctuations from 1999 to 2020. Our study found that from 1999 to 2020, the total SOC stock of the YRD decreased due to a large number of Wna converted to War. In addition, since the implementation of the WSRS in 2002, the new land area in the YRD has decreased. At the same time, due to seawater erosion, the total land area of the YRD has decreased. Further analysis showed that the SOC content of 0 ~ 10 cm soil in the YRD was much higher than that in other soil layers, indicating that surface soil protection was the most important factor in maintaining the stability of the soil carbon pool. This is because the root system of the dominant plant is mainly distributed in the depth of 0 ~ 10 cm soil layer, and the litter directly returns to the soil surface.

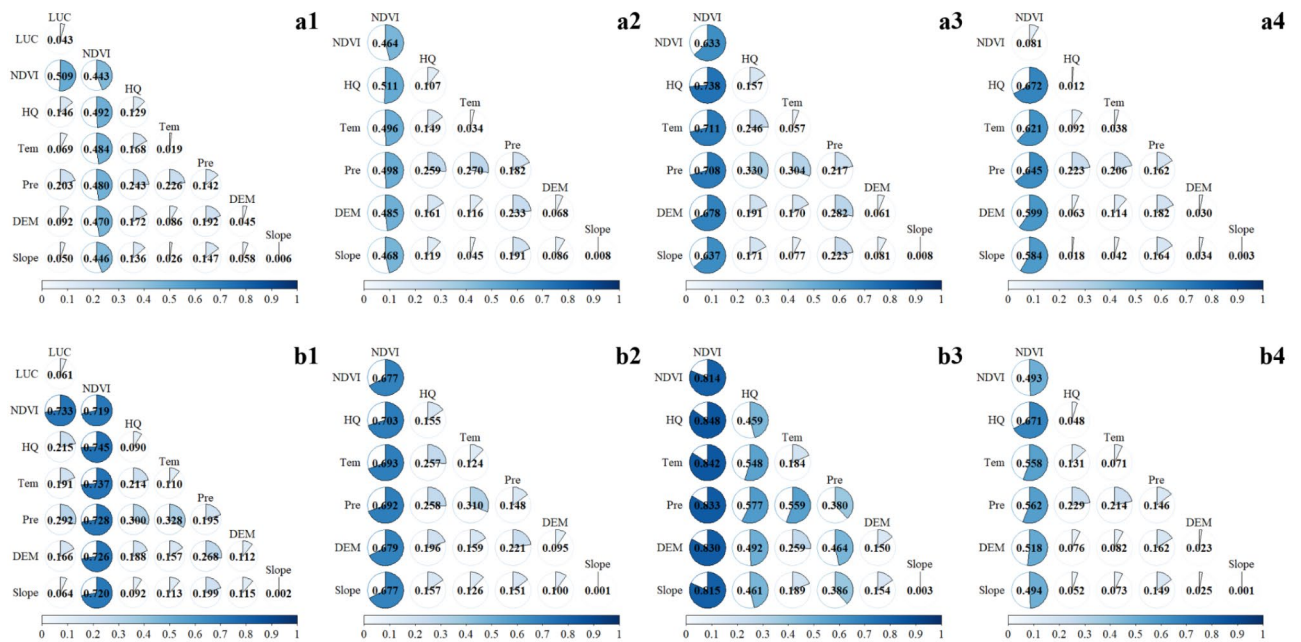


Fig. 8. FactorDetector and InteractionDetector results. **a1, a2, a3** and **a4** are the results of the GeoDetector model for YRD, Wna, War and Wno in 2000, respectively. **b1, b2, b3** and **b4** are the results of the GeoDetector model for YRD, Wna, War and Wno in 2000, respectively.

The carbon sink effect in the YRD showed a spatial distribution of “high in the center and low in the periphery” (Fig. 6), which is related to the spatial distribution of land use structure. Since 1976, when the YR was diverted, there has been a shortage of fresh water in the northern area, where the YR used to flow to the sea, and coastal erosion has occurred in many places. In addition, many wetland plant communities in the northern region also underwent reverse succession, showing wetland degradation. The coastal region of the YRD is distributed with large amounts of subsurface brine and hydrocarbon resources. In recent years, oil and gas extraction and continued development of aquaculture and salt production have led to severe land subsidence in the YRD³². These have caused parts of the YRD to become inundated as sea levels rise. At the same time, the wetland area and wetland type of the YRD have changed significantly due to intensive human activities, especially the WSRS implemented since 2002, which has had a significant impact on the morphology of the estuary⁶⁶. As a result, the area of Wna and Wno decreased, while the area of War increased. At the same time, the VCS rate per unit area of Wna, War and Wno all increased, but the growth rate of Wno was the fastest and that of Wna was the slowest. In summary, there are differences in the growth of LUCC and VCS rates in the YRD.

The frequency of extreme events resulting from global warming is likely to influence the distribution of groundwater and vegetation in the YRD, potentially impacting the carbon sinks present in this region⁶⁷. Furthermore, coast is endowed with substantial subterranean brine and oilfield resources in the YRD. However, excessive exploitation by humans will inevitably result in significant land subsidence⁶⁸. The combined effects of land subsidence and sea level rise will result in the YRD being at risk of being inundated by seawater, with a series of immeasurable social and economic impacts, particularly with regard to the region’s carbon cycle⁶⁹. Seawater inundation can firstly lead to a significant loss of carbon stocks and secondly to a reduction in vegetation cover, which in turn reduces the amount of VCS⁷⁰. As a result, to ensure the sustainable development of the YRD, the government should first reduce the unreasonable exploitation of underground brine and oil and gas to control land subsidence, and build more coastal dams in potentially submerged areas to prevent seawater intrusion²⁹. It should also strengthen the protection and repair of the existing dams. Therefore, in future projections of carbon stocks in the YRD, it is important to take into account climate change and sea level rise as well as sea water inundation that will result from land subsidence.

How the influencing factor affects the carbon sink effect?

Vegetation cover is the most critical factor affecting the ecosystem carbon sink effect. Vegetation index have been directly used to estimate NPP⁷¹. The YRD region consists mainly of wetlands with abundant surface water resources and groundwater resources, resulting in a smaller contribution of precipitation to VCS rate than NDVI^{37,38}. The VCS is affected by changes in precipitation, which will directly affect the photosynthesis of vegetation. Abundant rainfall promotes plant carbon sink, and both extreme rainfall and drought inhibit plant photosynthesis^{49,72}. The VCS estimation model is less affected by temperature changes. Rising temperature promote photosynthesis in plants, but also enhance respiration and transpiration. Frequent human activities have greatly affected the landscape pattern of coastal wetlands in the YRD, which in turn affects the HQ, indicating that LUCC and biodiversity has affected the carbon sink function of coastal wetland ecosystems⁷³.

Coastal wetlands provide diverse shelter and food sources for a large variety of terrestrial and marine species, creating unique food webs and high biodiversity⁴⁶. Greater biodiversity means greater vegetation cover, which means more carbon is fixed through photosynthesis^{33,74}. The overall topography of the YRD is relatively flat, and the influence of DEM and Slope is significantly less than other influencing factors.

The effect of precipitation on Wno was greater, while the effect of HQ on Wno was smaller. This is because the types of Wno are mainly impervious surfaces and drylands. Changes in the spatial pattern of Wno have obvious implications for VCS, particularly if large areas of Wna are converted to Wno and the carbon balance of regional ecosystems can be altered. The influence of temperature on Wna is significantly greater than that of other LUC types. This is because temperature mainly affects photosynthesis and respiration of plants, and Wna has the most vegetation cover. Furthermore, climate warming will reduce the resistance and resilience of Wna⁷⁵.

How to improve the carbon sink function?

We demonstrated that vegetation cover defines the spatial pattern of carbon sink in the YRD, which differs from other studies conducted on a large scale, emphasizing the significance of climatic factors, such as temperature and precipitation. In the context of global warming and frequent extreme events such as droughts and rainstorms, the YRD region may have to face problems such as increasing soil salinity and insufficient availability of fresh water resources. The lack of an optimal restoration type that is universally applicable to all climates is coupled with the high cost of human-assisted ecological restoration¹³. Thus, management needs to select the appropriate type of restored vegetation based on local constraints such as precipitation and groundwater salinity to achieve optimal growth of carbon sink function. Quantitative methods are used to further determine where, how much, and what species of plants are recommended for restoration⁷⁶.

Meanwhile, the spatiotemporal evolution of wetland patterns caused by natural evolution and human disturbance led to the spatiotemporal evolution of VCS and SOC patterns in the YRD. This study showed that the vegetation cover of coastal wetlands in the YRD has increased significantly since 2000, improving the carbon sink function. However, the change of wetland pattern, especially the reduction of Wna, makes the mechanism of VCS in the YRD unstable. In future wetland conservation, we should not only aim to increase vegetation cover, but also pay attention to biodiversity. In the past, we have pursued increasing vegetation cover while neglecting to protect biodiversity. Increasing vegetation cover will significantly increase the carbon sink function of the ecosystem, but if the biodiversity is neglected, the ecosystem will become fragile. Our results also showed that the synergistic effect of vegetation cover and biodiversity on ecosystem carbon sink function has become the strongest. In the context of sea level rise, future efforts to enhance the carbon sink function of coastal wetlands should focus on improving ecosystem stability through measures such as biodiversity conservation.

The Chinese government is paying attention to the protection of coastal wetlands. By the end of 2018, it had invested about \$1.5 billion to restore 3,549 ha of coastal wetlands⁷⁷. Especially in the YRD, China established the YRD National Natural Reserve in 1992 to protect the emerging wetland system and rare and endangered birds (Fig. 1d). The results can be used as a scientific reference for ecological protection and high-quality development in the YRD, as well as for environmental protection and sustainable management of coastal wetlands. This work reminds local governments to protect the Wna of the YRD by formulating reasonable policies. At the same time, the diversion of water and sand should be weighed up to avoid the disappearance of the YRD.

Uncertainties and future works

We applied the CASA model in YRD to reveal the VCS as a carbon sink. Under the influence of human beings, the coastal wetland ecosystem has undergone significant changes, which is a complex process and has affects the carbon cycle of the regional ecosystem, increasing the uncertainty. The complexity of the coastal wetland ecosystem merits further investigation.

In this paper, NDVI is calculated using the MOD13Q1 dataset, which has a spatial resolution of 250 m; the spatial resolution of the LUC data and the HQ simulated by the InVest - habitat quality model is 30 m; the spatial resolution of temperature and precipitation data is 1 km. As the individual data have inconsistent spatial resolution, resampling is required before combining them, and errors can occur. Secondly, the Kriging interpolation results of the monitoring data from the stations in the study area may differ from the actual solar radiation. This paper does not use land use data for consecutive years, which may affect the accuracy of the simulation. Since land use change is a slow process, it can be assumed that the selection of discontinuous land-use data has little effect on the modelling of NPP. In future studies, land use with higher spatiotemporal resolution could be used to further improve accuracy. Besides, in some of the analyses, we calculated the 1999 LUCC data as if it was 2000, which may cause some uncertainty.

In this paper, we only estimated the SOC stock at a depth of one meter in the study area, whereas the SOC stock at the first meter depth only accounts for about 54% of the total SOC stock^{14,17}. Future studies should explore deeper SOC stock. In addition, our approach to estimating SOC introduces uncertainty. We measured the SOC content of different LUC types at different soil layers through soil sampling and obtained LUC type interpretation data at different times with the help of remote sensing interpretation. However, the SOC stocks calculated using only 2002 and 2003 data create some uncertainty. Meanwhile, there is a time lag between the transition of SOC stock and the change of LUC type, and the change of SOC stock obtained by this method over 20 years has a certain error.

In comparison with other studies, the values of our NPP were within a reasonable range (Table 1). Furthermore, in 2009, the SOC stock of the YRD was 7.1661 Tg C, among which the SOC stock of 0 ~ 30 cm was 3.6896 Tg C, similar to the research conclusion (3.5451 Tg C) of Yu et al.⁴⁴.

Conclusion

In this study, we obtained the spatiotemporal patterns of SOC and VCS in the YRD, as well as the effects of various influencing factors on carbon sinks. The results showed that: (1) From 1999 to 2020, the area of natural-wetlands and non-wetlands decreased, while the area of artificial wetlands increased. (2) The SOC stock in the 0–100 cm depth in 1999 and 2020 were about 7.8871 Tg C and 7.0521 Tg C, respectively. The amount of VCS increased from 0.2309 Tg C in 2000 to 0.3681 Tg C in 2020, with a significant annual increase of 6532 Mg C. In the past 21 years, the total carbon sink in the YRD was 6.0952 Tg C. The amount of VCS was equivalent to 2.93% of SOC stock in 1999, rising to 5.22% by 2020. (3) Vegetation cover has the greatest influence on the carbon sink function in the YRD, followed by precipitation and biodiversity. From 2000 to 2020, the effect of biodiversity on the carbon sinks of natural-wetlands and artificial wetlands increased. The synergistic effect of wetland type and vegetation cover on carbon sink effect was replaced by the synergistic effect of biodiversity and vegetation cover.

Data availability

The datasets used and/or analysed during the current study available from the corresponding author on reasonable request.

Received: 13 July 2024; Accepted: 15 November 2024

Published online: 22 November 2024

References

- Lee, H. et al. IPCC, : Climate Change 2023: Synthesis Report, Summary for Policymakers. Contribution of Working Groups I, II and III to the Sixth Assessment Report of the Intergovernmental Panel on Climate Change. *IPCC, Geneva, Switzerland*, (2023). <https://doi.org/10.59327/IPCC/AR6-9789291691647.001> (2023).
- Schuerch, M. et al. Future response of global coastal wetlands to sea-level rise. *Nature*. **561**, 231–234. <https://doi.org/10.1038/s41586-018-0476-5> (2018).
- Xu, X. Frequent occurrence of extreme weather and out-of-balance climate systems. *Innov. Geoscience*. **2**, 100049. <https://doi.org/10.59717/j.xinn-geo.2024.100049> (2024).
- Saintilan, N. et al. Widespread retreat of coastal habitat is likely at warming levels above 1.5 degrees C. *Nature*. **621**, 112–119. <https://doi.org/10.1038/s41586-023-06448-z> (2023).
- Chen, Z., Wang, W., Forzieri, G. & Cescatti, A. Transition from positive to negative indirect CO₂ effects on the vegetation carbon uptake. *Nat. Commun.* **15**, 1500. <https://doi.org/10.1038/s41467-024-45957-x> (2024).
- Pan, Y. et al. The enduring world forest carbon sink. *Nature*. **631**, 563–569. <https://doi.org/10.1038/s41586-024-07602-x> (2024).
- Piao, S., He, Y., Wang, X. & Chen, F. Estimation of China's terrestrial ecosystem carbon sink: methods, progress and prospects. *Sci. China Earth Sci.* **65**, 641–651. <https://doi.org/10.1007/s11430-021-9892-6> (2022).
- Mitsch, W. J. et al. Wetlands, carbon, and climate change. *Landscape Ecol.* **28**, 583–597. <https://doi.org/10.1007/s10980-012-9758-8> (2012).
- Ren, Y. et al. China's wetland soil organic carbon pool: New estimation on pool size, change, and trajectory. *Glob Chang. Biol.* **29**, 6139–6156. <https://doi.org/10.1111/gcb.16923> (2023).
- Dang, C. et al. Global vegetation productivity increased in response to COVID-19 restrictions. *Geo-spatial Inform. Sci.* 1–14. <https://doi.org/10.1080/10095020.2023.2300842> (2024).
- Tong, X. et al. Increased vegetation growth and carbon stock in China karst via ecological engineering. *Nat. Sustain.* **1**, 44–50. <https://doi.org/10.1038/s41893-017-0004-x> (2018).
- Zhang, M. et al. How ecological restoration alters ecosystem services: an analysis of vegetation carbon sequestration in the karst area of northwest Guangxi, China. *Environ. Earth Sci.* **74**, 5307–5317. <https://doi.org/10.1007/s12665-015-4542-0> (2015).
- Feng, X., Fu, B., Lu, N., Zeng, Y. & Wu, B. How ecological restoration alters ecosystem services: an analysis of carbon sequestration in China's Loess Plateau. *Sci. Rep.* **3**, 1–5. <https://doi.org/10.1038/srep02846> (2013).
- Jobbágy, E. G. & Jackson, R. B. The vertical distribution of soil organic carbon and its relation to climate and vegetation. *Ecological applications*. *Ecol. Appl.* **10**, 423–436. [https://doi.org/10.1890/1051-0761\(2000\)010\[0423:TVDOSO\]2.0.CO;2](https://doi.org/10.1890/1051-0761(2000)010[0423:TVDOSO]2.0.CO;2) (2000).
- Stockmann, U. et al. Global soil organic carbon assessment. *Global Food Secur.* **6**, 9–16. <https://doi.org/10.1016/j.gfs.2015.07.001> (2015).
- Stockmann, U. et al. The knowns, known unknowns and unknowns of sequestration of soil organic carbon. *Agric. Ecosyst. Environ.* **164**, 80–99. <https://doi.org/10.1016/j.agee.2012.10.001> (2013).
- Guo, L. B. & Gifford, R. M. J. G. c. b. soil carbon stocks and land use change: a meta analysis. *Glob. Change Biol.* **8**, 345–360. <https://doi.org/10.1046/j.1354-1013.2002.00486.x> (2002).
- Xia, S. et al. Storage, patterns and influencing factors for soil organic carbon in coastal wetlands of China. *Glob Chang. Biol.* **28**, 6065–6085. <https://doi.org/10.1111/gcb.16325> (2022).
- McLeod, E. et al. A blueprint for blue carbon: toward an improved understanding of the role of vegetated coastal habitats in sequestering CO₂. *Front. Ecol. Environ.* **9**, 552–560. <https://doi.org/10.1890/110004> (2011).
- Dodla, S. K., Wang, J. J. & Delaune, R. D. Characterization of labile organic carbon in coastal wetland soils of the Mississippi River deltaic plain: relationships to carbon functionalities. *Sci. Total Environ.* **435**, 151–158. <https://doi.org/10.1016/j.scitotenv.2012.06.090> (2012).
- Amthor, J. & Huston, M. J. O. T. M. Terrestrial ecosystem responses to global change: A research strategy. *ORNL Tech. Memorandum* **27**, 37. Report number: ORNL/TM-1998/27 (1998).
- Wang, J. et al. Large Chinese land carbon sink estimated from atmospheric carbon dioxide data. *Nature*. **586**, 720–723. <https://doi.org/10.1038/s41586-020-2849-9> (2020).
- Wang, Y. et al. The size of the land carbon sink in China. *Nature*. **603**, E7–E9. <https://doi.org/10.1038/s41586-021-04255-y> (2022).
- Wang, J. et al. Reply to: 'The size of the land carbon sink in China. *Nature*. **603**, E10–E12. <https://doi.org/10.1038/s41586-021-04256-x> (2022).
- Cao, L. et al. Research progresses in carbon budget and carbon cycle of the coastal salt marshes in China. *Acta Ecol. Sin.* **33**, 5141–5152. <https://doi.org/10.5846/stxb201206030803> (2013). (In Chinese).
- Lu, M. et al. Anthropogenic disturbances caused declines in the wetland area and carbon pool in China during the last four decades. *Glob Chang. Biol.* **27**, 3837–3845. <https://doi.org/10.1111/gcb.15671> (2021).
- Wang, H. et al. Impacts of the dam-orientated water-sediment regulation scheme on the lower reaches and delta of the Yellow River (Huanghe): a review. *Glob. Planet Change*. **157**, 93–113. <https://doi.org/10.1016/j.gloplacha.2017.08.005> (2017).
- Wang, H., Yang, Z., Bi, N. & Li, H. J. C. S. B. Rapid shifts of the river plume pathway off the Huanghe (Yellow) River mouth in response to water-sediment regulation scheme in 2005. *Chin. Sci. Bull.* **50**, 2878–2884. <https://doi.org/10.1360/982005-1196> (2005).

29. Tang, Z. et al. Projections of land use/cover change and habitat quality in the model area of Yellow River delta by coupling land subsidence and sea level rise. *Ecol. Ind.* **158**, 111394. <https://doi.org/10.1016/j.ecolind.2023.111394> (2024).
30. Bai, J., Xiao, R., Zhang, K. & Gao, H. Arsenic and heavy metal pollution in wetland soils from tidal freshwater and salt marshes before and after the flow-sediment regulation regime in the Yellow River Delta, China. *J. Hydrol.* **450**, 244–253. <https://doi.org/10.1016/j.jhydrol.2012.05.006> (2012).
31. Su, L. et al. Effects of groundwater depth on root growth of *Tamarix chinensis* in the Yellow River Delta. *Acta Ecol. Sin.* **41**, 3794–3804. <https://doi.org/10.5846/stxb202008082069> (2021). (In Chinese).
32. Liu, Y. et al. Land subsidence of the Yellow River Delta in China driven by river sediment compaction. *Sci. Total Environ.* **750**, 142165. <https://doi.org/10.1016/j.scitotenv.2020.142165> (2021).
33. Xie, X., Li, X., Bai, J. & Zhi, L. Variations of Aboveground Biomass of 4 kinds of typical plants with Surface Elevation of wetlands in the Yellow River Delta. *Wetland Sci.* **19**, 226–231. <https://doi.org/10.13248/j.cnki.wetlandsci.2021.02.010> (2021).
34. Zhang, X., Zhaohui, Z., Zongjun, X., Xuejing, H. & Qingfang, C. On the relation between carbon storage and reinforced fixation of the coastal wetland vegetation in the Yellow River delta area. *J. Saf. Environ.* **12**, 145–149. <https://doi.org/10.3969/j.issn.1009-6094.2012.06.031> (2012). (In Chinese).
35. Chi, Y. et al. Spatio-temporal characteristics and main influencing factors of vegetation net primary productivity in the Yellow River Delta in recent 30 years. *Acta Ecol. Sin.* **38**, 2683–2697. <https://doi.org/10.5846/stxb201705301000> (2018). (In Chinese).
36. Jiang, R., Li, X., Zhu, Y. & Zhang, Z. Spatial-temporal variation of NPP and NDVI correlation in wetland of Yellow River Delta based on MODIS data. *Acta Ecol. Sin.* **31**, 6708–6716 (2011). (In Chinese).
37. Lu, G., Han, M., Zehua, X., Jiqian, Z. & Niu, X. Spatiotemporal variations of net primary productivity in new wetlands of the Yellow River Delta. *Chin. J. Ecol.* **38**, 1113–1122. <https://doi.org/10.13292/j.1000-4890.201904.036> (2019).
38. Zhang, X. et al. Quantifying the contributions of climate change and human activities to vegetation dynamic changes in the Yellow River Delta. *Acta Sci. Circum.* **42**, 56–69. <https://doi.org/10.13671/j.hjkxxb.2021.0492> (2022).
39. Wei, S. et al. Effect of tidal flooding on ecosystem CO₂ and CH₄ fluxes in a salt marsh in the Yellow River Delta. *Estuar. Coast. Shelf Sci.* **232**, 106512. <https://doi.org/10.1016/j.ecss.2019.106512> (2020).
40. Song, H. & Sun, Z. Temporal variations and bioaccumulation of heavy metals in different Suaeda salsa marshes of the Yellow River Estuary, China. *Environ. Sci. Pollut. Res. Int.* **21**, 14174–14187. <https://doi.org/10.1007/s11356-014-3296-7> (2014).
41. Qu, W. et al. Nitrogen input in different chemical forms and levels stimulates soil organic carbon decomposition in a coastal wetland. *Catena.* **194**, 104672. <https://doi.org/10.1016/j.catena.2020.104672> (2020).
42. Chen, Y. et al. Modeling impacts of changes in Water Level on net ecosystem CO₂ exchange in a Coastal Wetland of the Yellow River Delta Based on DNDC Model. *Ecol. Environ. Sci.* **30**, 254–263. <https://doi.org/10.16258/j.cnki.1674-5906.2021.02.004> (2021).
43. Wang, J., Bai, J., Zhao, Q., Lu, Q. & Xia, Z. Five-year changes in soil organic carbon and total nitrogen in coastal wetlands affected by flow-sediment regulation in a Chinese delta. *Sci. Rep.* **6**, 21137. <https://doi.org/10.1038/srep21137> (2016).
44. Yu, J. et al. Soil organic carbon storage changes in coastal wetlands of the modern Yellow River Delta from 2000 to 2009. *Biogeosciences.* **9**, 2325–2331. <https://doi.org/10.5194/bg-9-2325-2012> (2012).
45. Yu, J. et al. Estimation of Soil Organic Carbon Storage in Coastal Wetlands of Modern Yellow River Delta based on Landscape Pattern. *Wetland Sci.* **11**, 1–6. <https://doi.org/10.13248/j.cnki.wetlandsci.2013.01.006> (2013).
46. Song, H., Liu, X., Wang, L., Yu, W. & Dong, B. Spatial and temporal distribution of Soil Organic Carbon in Vegetation Communities of the Yellow River Delta under different disturbance levels. *J. Soil Water Conserv.* **32**, 190–196. <https://doi.org/10.13870/j.cnki.stb.cxb.2018.01.030> (2018). (In Chinese).
47. Ye, S. et al. Carbon Sequestration and Soil Accretion in Coastal Wetland communities of the Yellow River Delta and Liaohe Delta, China. *Estuaries Coasts.* **38**, 1885–1897. <https://doi.org/10.1007/s12237-014-9927-x> (2015).
48. Du, Z., Dong, H., Jing, D., Ma, B. & Liu, F. Effects of long term plantations on Soil Organic Carbon Pool in Yellow River Delta. *Bull. Soil Water Conserv.* **36**, 56–61. <https://doi.org/10.13961/j.cnki.stbctb.2016.05.017> (2016).
49. Shao, P., Han, H. & Sun, J. Effects of wetland degradation and restoration on soil organic carbon content and infrared carbon compounds of *Tamarix chinensis* Woodland in the Yellow River Delta. *Chin. J. Ecol.* **41**, 1258–1265. <https://doi.org/10.13292/j.1000-4890.202207.026> (2022).
50. Li, J. et al. Effects of drying-rewetting frequency on Vertical and lateral loss of Soil Organic Carbon in a Tidal Salt Marsh. *Wetlands.* **40**, 1433–1443. <https://doi.org/10.1007/s13157-020-01286-5> (2020).
51. Jiao, S. et al. N, and P distribution as affected by plant communities in the Yellow River Delta, China. *PLoS One.* **14**, e0226887. <https://doi.org/10.1371/journal.pone.0226887> (2019).
52. Jiao, S. et al. Variation of soil organic carbon and physical properties in relation to land uses in the Yellow River Delta, China. *Sci. Rep.* **10**, 20317. <https://doi.org/10.1038/s41598-020-77303-8> (2020).
53. Li, Y. Evolution process and its driving mechanism of coastal wetlands in the Yellow River Delta. *University of Chinese Academy of Science*. CSTR:35001.37.01.33190.20140024 (2014). (In Chinese).
54. He, Q., Wang, M., Liu, K., Li, K. & Jiang, Z. GPRChinaTemp1km: a high-resolution monthly air temperature dataset for China (1951–2020) based on machine learning. *Earth Syst. Sci. Data Discuss.* 1–29. <https://doi.org/10.5194/essd-2021-267> (2021).
55. Qu, L., Zhu, Q., Zhu, C. & Zhang, J. Monthly precipitation data set with 1 km resolution in China from 1960 to 2020. *Sci. Data Bank.* <https://doi.org/10.11922/sciencedb.01607> (2021).
56. Wu, H., Guo, Z. & Peng, C. Distribution and storage of soil organic carbon in China. *Glob. Biogeochem. Cycles.* **17**, 1048. <https://doi.org/10.1029/2001gb001844> (2003).
57. Zhao, Q. et al. Soil organic carbon content and stock in wetlands with different hydrologic conditions in the Yellow River Delta, China. *Ecohydrol. Hydrobiol.* **20**, 537–547. <https://doi.org/10.1016/j.ecohyd.2019.10.008> (2020).
58. Wang, S., Zhou, C., Li, K., Zhu, S. & Huang, F. Analysis on spatial distribution characteristics of Soil Organic Carbon Reservoir in China. *Acta Ecol. Sin.* **55**, 533–544. https://doi.org/10.1007/978-1-4615-0793-2_1 (2000). (In Chinese).
59. Wen, Q. Composition, formation and decomposition of soil organic matter. *Soils.* **04**, 121–129. <https://doi.org/10.13758/j.cnki.tr.1984> (1984). (In Chinese).
60. Potte, C. S. et al. Terrestrial ecosystem production a process model based on global satellite and surface data. *Glob. Biogeochem. Cycles.* **7**, 811–841. <https://doi.org/10.1029/93GB02725> (1993).
61. Xu, Q., Dong, Y. & Yang, R. Influence of different geographical factors on carbon sink functions in the Pearl River Delta. *Sci. Rep.* **7**, 110. <https://doi.org/10.1038/s41598-017-00158-z> (2017).
62. Yang, D. et al. Quantifying the influence of natural and socioeconomic factors and their interactive impact on PM_{2.5} pollution in China. *Environ. Pollut.* **241**, 475–483. <https://doi.org/10.1016/j.envpol.2018.05.043> (2018).
63. Fei, X., Lou, Z., Xiao, R., Ren, Z. & Lv, X. Contamination assessment and source apportionment of heavy metals in agricultural soil through the synthesis of PMF and GeogDetector models. *Sci. Total Environ.* **747**, 141293. <https://doi.org/10.1016/j.scitotenv.2020.141293> (2020).
64. Wang, J. & Hu, Y. Environmental health risk detection with GeogDetector. *Environ. Model. Softw.* **33**, 114–115. <https://doi.org/10.1016/j.envsoft.2012.01.015> (2012).
65. Wang, J., Xu, C. & Geodetector Principle and prospective. *Acta Geogr. Sin.* **72**, 116–134. <https://doi.org/10.11821/dlxb201701010> (2017). (In Chinese).
66. Wang, H. et al. Recent changes in sediment delivery by the Huanghe (Yellow River) to the sea: causes and environmental implications in its estuary. *J. Hydrol.* **391**, 302–313. <https://doi.org/10.1016/j.jhydrol.2010.07.030> (2010).

67. Luo, F. et al. Estuarine groundwater level response to and recovery from extreme precipitation events: Typhoon Lekima in the Yellow River Delta. *J. Hydrol.* **632**, 130918. <https://doi.org/10.1016/j.jhydrol.2024.130918> (2024).
68. Wang, G. et al. InSAR and machine learning reveal new understanding of coastal subsidence risk in the Yellow River Delta, China. *Sci. Total Environ.* **915**, 170203. <https://doi.org/10.1016/j.scitotenv.2024.170203> (2024).
69. Li, P., Wang, G., Liang, C., Wang, H. & Li, Z. InSAR-Derived Coastal Subsidence reveals new inundation scenarios over the Yellow River Delta. *IEEE J. Sel. Top. Appl. Earth Observations Remote Sens.* **16**, 8431–8441. <https://doi.org/10.1109/jstars.2023.3272782> (2023).
70. Tang, Z. et al. Carbon stocks in coastal wetlands of the Yellow River Delta and their response to future multi-scenarios. *Acta Ecol. Sin.* **44**, 3280–3292. <https://doi.org/10.20103/i.stxb.202308211801> (2024). (In Chinese).
71. Jiang, H., Apps, M. J., Zhang, Y., Peng, C. & Woodard, P. M. Modelling the spatial pattern of net primary productivity in Chinese forests. *Ecol. Model.* **122**, 275–288. [https://doi.org/10.1016/S0304-3800\(99\)00142-8](https://doi.org/10.1016/S0304-3800(99)00142-8) (1999).
72. Chu, X. et al. Changes in plant biomass induced by soil moisture variability drive interannual variation in the net ecosystem CO₂ exchange over a reclaimed coastal wetland. *Agric. For. Meteorol.* **264**, 138–148. <https://doi.org/10.1016/j.agrformet.2018.09.013> (2019).
73. Huang, Y. et al. Habitat quality evaluation and pattern simulation of coastal salt marsh wetlands. *Sci. Total Environ.* **945**, 174003. <https://doi.org/10.1016/j.scitotenv.2024.174003> (2024).
74. Schulze, E. D. Biological control of the terrestrial carbon sink. *Biogeosciences*. **3**, 147–166. <https://doi.org/10.5194/bg-3-147-2006> (2006).
75. Sun, B. et al. Experimental warming reduces ecosystem resistance and resilience to severe flooding in a wetland. *Sci. Adv.* **8**, eabl9526. <https://doi.org/10.1126/sciadv.abl95> (2020).
76. Yu, S. et al. A quantitative approach for offsetting the coastal reclamation impacts on multiple ecosystem services in the Yellow River Delta. *Ecosyst. Serv.* **52**, 101382. <https://doi.org/10.1016/j.ecoser.2021.101382> (2021).
77. Wang, X., Yan, F., Vincent, L. & Su, F. Restore China's coastline from the ground up. *Science*. **377**, 1164. <https://doi.org/10.1126/science.ade3911> (2022).

Author contributions

D.W., and Z.Z.: Conceptualization, Supervision, Funding acquisition. Z.T.: Methodology, Validation, Visualization, Writing - Original Draft, Writing - Review & Editing. F.L.: Supervision, Writing - Review & Editing. X.T., X.B., R.N.: Supervision. J.L.: Writing - Review & Editing. All authors commented on previous versions of the manuscript. All authors read and approved the final.

This work was supported by the seed project of Yantai Institute of Coastal Zone Research, Chinese Academy of Sciences (No. YIC E351030601), the National Natural Science Foundation of China (No.41001360, 31870468 and 42206240) and the Natural Science Foundation of Shandong Province (ZR2023MC002). We would like to thank the Yellow River Delta Field Observation and Research Station of Coastal Wetland Ecosystem, Chinese Academy of Sciences for their help in field work.

Declarations

Competing interests

The authors declare no competing interests.

Additional information

Correspondence and requests for materials should be addressed to D.W.

Reprints and permissions information is available at www.nature.com/reprints.

Publisher's note Springer Nature remains neutral with regard to jurisdictional claims in published maps and institutional affiliations.

Open Access This article is licensed under a Creative Commons Attribution-NonCommercial-NoDerivatives 4.0 International License, which permits any non-commercial use, sharing, distribution and reproduction in any medium or format, as long as you give appropriate credit to the original author(s) and the source, provide a link to the Creative Commons licence, and indicate if you modified the licensed material. You do not have permission under this licence to share adapted material derived from this article or parts of it. The images or other third party material in this article are included in the article's Creative Commons licence, unless indicated otherwise in a credit line to the material. If material is not included in the article's Creative Commons licence and your intended use is not permitted by statutory regulation or exceeds the permitted use, you will need to obtain permission directly from the copyright holder. To view a copy of this licence, visit <http://creativecommons.org/licenses/by-nc-nd/4.0/>.

© The Author(s) 2024